

## INVESTIGATION OF THE MICROPHYSICAL CHARACTERISTICS OF AEROSOLS BY THE METHOD OF ELECTRODYNAMIC SUSPENSION OF PARTICLES.

### 1. STRUCTURE OF THE EDS AND DETERMINATION OF THE DRAG FORCE OF MICROPARTICLES

V. A. Runkov, P. E. Suetin, and  
S. A. Beresnev

UDC 531.75+541.18

*This paper describes the structure of an electrodynamic suspension (EDS) with flat electrodes for investigating a complex of characteristics of charged microparticles and the surrounding gas. A linear theory of oscillatory motion of a microparticle in the EDS volume has been developed and analytical expressions for the oscillation amplitude and the center of oscillation of a particle depending on the electrode voltage value have been obtained. The stability boundary of motion of particles of various substances for the EDS of the given configuration has been determined theoretically. For the first time the dynamic behavior of aerosols in the EDS in a wide range of change in the surrounding gas pressure (Knudsen number) has been studied experimentally, in particular, data for the drag force of a particle have been obtained. Comparison between the experimental and theoretical data has been made.*

**Introduction.** It is highly convenient to make laboratory investigations of the microphysical properties of atmospheric aerosols by levitating single particles (or a small collective of particles) in the measuring cell under the action of forces of various nature. The use of this method is promising for investigating the processes of interaction between a low-intensity electromagnetic radiation and particles of various substances in a wide range of their sizes (from 1 to 100  $\mu\text{m}$ ) at various temperatures and pressures of the surrounding gas (up to  $10^{-2}$  torr). Obviously, such conditions provide a fairly complete and correct model of the behavior of atmospheric aerosols at high altitudes (in the stratosphere and mesosphere) in the field of solar radiation not only in terms of the Knudsen number, but in terms of the value of the diffraction parameter as well.

At the present time, the most popular technique for levitating charged microparticles is their confinement in the EDS volume, where a combined action of constant and variable electric fields is used [1]. In this case, various configurations of EDS electrodes are used — from the most complicated ones (e.g., bihyperbolic electrodes in [2] and octupole ones in [3]) to fairly simple electrodes (coaxial rings-electrodes in [4, 5]). The most comprehensive review of the state-of-the-art of the investigations in this field is given in [1].

The present paper describes the structure and the results of the initial studies with aerosol microparticles for the original structure of an EDS with ring electrodes for the variable electric field and flat disk electrodes for the constant electric field. A suspension with such a configuration of electrodes has a number of important advantages over other realizations. First, the best conditions for observing the particle motion in the chamber volume are provided for it; second, it permits realizing a wider set of vertical force actions on the microparticle as compared to other types of suspensions; and, third, the given configuration of electrodes admits a fairly easy calculation of electric field strengths in the EDS volume, which is necessary for analyzing experimental results. Unlike the other known realizations of EDSs with this configuration of electrodes [4, 5], the measuring cell is in the vacuum chamber, permitting working with gas pressures of up to  $10^{-2}$  torr, which corresponds to altitudes of the terrestrial atmosphere up to 80 km. Note that the proposed structure has a number of advantages over the EDS used by the authors earlier [6] (in particular, a more stable confinement of particles in the measuring volume is provided).

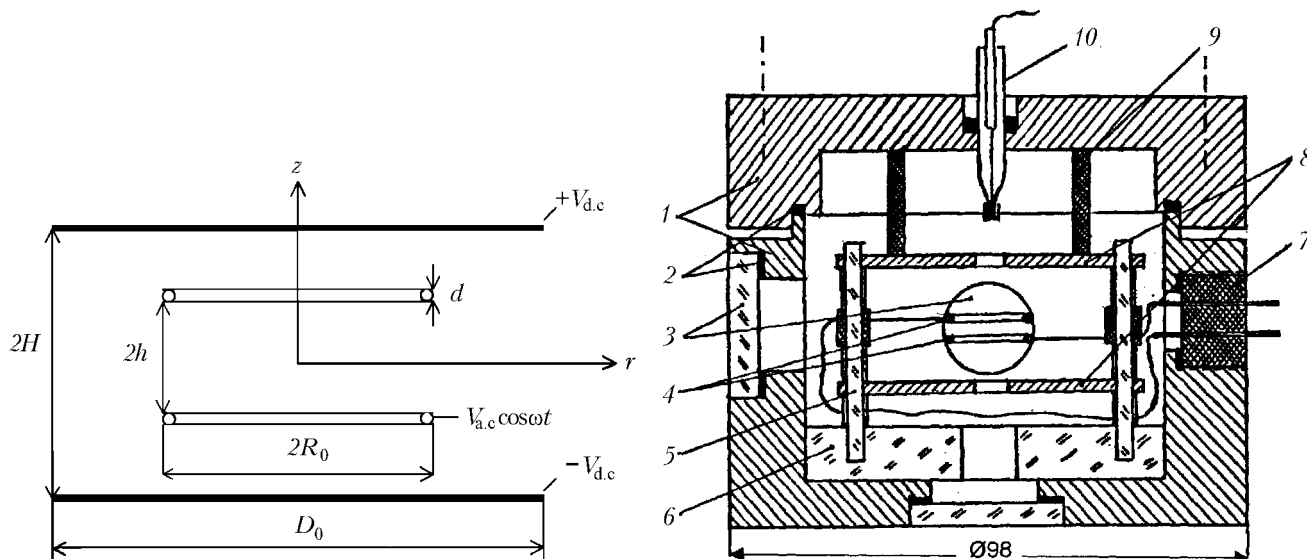


Fig. 1. Configuration of electrodes in the EDS.

Fig. 2. Working chamber of the experimental set (vertical section): 1) brass casing; 2) rubber gaskets; 3) viewing window; 4) ring electrodes creating a variable electric field; 5) glass posts; 6) EDS base; 7) electrical inputs; 8) ring electrodes (disks) creating a constant electric field; 9) press plug; 10) ionizer.

**Description of the EDS and Experimental Procedure.** Figure 1 shows the arrangement of the electrodynamic suspension electrodes and Figure 2 gives the vertical section of the chamber of the experimental set based on an EDS with plane-parallel electrodes. The set consists of a brass chamber 1 inside of which there are two copper rings 4 used to create a variable electric field and two aluminum disks 8 by means of which a constant electric field is created. The internal diameter of the chamber is 98 mm and its height is equal to 80 mm. The rings are made of copper wire of thickness  $d = 1$  mm and have a radius  $R_0 = 6.7$  mm. The disk diameter  $D_0 = 60$  mm and the thickness is 3 mm. The distance between the rings is  $2h = 4$  mm and the distance between the disks is  $2H = 28$  mm. The chamber has six holes used to inject particles, for electrical inputs, to illuminate the measuring volume, enter external radiation, evacuate the chamber, and observe the particle. In the upper cover, an ionizer 10 designed to charge and inject aerosol particles into the chamber is located. The ionizer is a glass pipette to whose tip a grounded ring electrode is attached. Inside the pipette there is a needle to which a high negative voltage ( $-4.5$  kV) is applied. A small amount of powder from the particles being investigated is placed in the ionizer. When the needle approaches the pipette tip, there occurs an electric discharge, which provides the charging of particles and their ejection into the chamber.

To confine a charged particle inside the EDS, the following method was used. A group of several particles upon leaving the ionizer got into the working chamber. Initially, only a.c. voltage was fed to the ring electrodes. Part of the incident particles was captured by the variable electric field in different positions between the rings. Then, decreasing the value of a.c. voltage, we managed to make all particles, except one, settle out on the rings or the chamber walls. Then the a.c. voltage was increased and the particle occupied a position on the EDS axis below its geometric center. In so doing, the particle executed oscillations along the vertical axis of the EDS. Varying the d.c. voltage on the disk, one can place the particle in the EDS center, where it will remain in a stable position for a long time at a certain value of the a.c. voltage.

**Brief Theory of the Electrodynamic Suspension.** To use the EDS for investigating various physical processes with atmospheric aerosols, it is necessary to solve the problem on the charged particle motion in electric fields inside the suspension volume. The equation of a fairly large particle (which corresponds to the efficiency condition of the Stokes formula) for the axial component is of the form

$$m \frac{d^2 z}{dt^2} + 6\pi\eta R_p \frac{dz}{dt} - qE_{a.c.} = q(E_{d.c.} - E_{d.c.}(0)). \quad (1)$$

TABLE 1. Particle Sizes Determined from Experiments on the Investigation of the Stability Boundary (Fig. 3)

Particle number	Particle substance	$R_p \pm \Delta R_p, \mu\text{m}$
1	Lycopodium spores	$10.7 \pm 0.2$
2	»	$11.1 \pm 0.2$
3	»	$12.3 \pm 0.2$
4	»	$15.5 \pm 0.3$
5	Nickel particle	$4.8 \pm 0.1$
6	»	$5.1 \pm 0.1$
7	Iron particle	$8.2 \pm 0.2$
8	»	$9.0 \pm 0.2$
9	»	$9.2 \pm 0.2$
10	Copper particle	$8.5 \pm 0.2$
11	»	$8.7 \pm 0.2$
12	»	$9.7 \pm 0.2$
13	Titanium particle	$8.9 \pm 0.2$
14	»	$11.6 \pm 0.2$
15	»	$12.3 \pm 0.2$

Here  $E_{d.c}(0)$  is the strength of the constant electric field providing confinement of the particle at the EDS center where the condition of equality of gravity and electrostatic force

$$qE_{d.c}(0) = mg \quad (2)$$

is met. Taking into account the form of the solution of the Laplace equation for the electric potential in the volume of an EDS of a given configuration [4, 5], we can write Eq. (1) in the form

$$\frac{d^2 z}{dt^2} + A \frac{dz}{dt} - Bz \cos t = D, \quad (3)$$

$$A = \frac{6\pi\eta R_p}{m\omega}, \quad B = \frac{g}{\omega^2} \frac{C_{a.c.}}{C_0} \frac{V_{a.c.}}{V_{d.c}(0)}, \quad D = \frac{g}{\omega^2} \left( \frac{V_{d.c.}}{V_{d.c}(0)} - 1 \right), \quad (4)$$

where  $V_{a.c.}$  and  $V_{d.c.}$  are the variable and constant fields on the electrodes,  $V_{d.c}(0)$  is the d.c. voltage at the EDS center, and  $C_{a.c.}$  and  $C_0$  are the geometric constants determined by the size and shape of the electrodes. For the EDS configuration used, the ratio of the geometric constants was estimated as  $C_{a.c.}/C_0 = 603.5 \text{ m}^{-1}$ ; the geometric constant  $C_{a.c.}$  for the ring lasers thereby was calculated by the method of [4] and  $C_0$  was calculated from the estimate of the capacity of the flat capacitor with regard for the end effects.

The nonlinear equation (3) at  $D = 0$  can be reduced to the Mathieu equation describing the nonlinear processes in electrical and mechanical systems. Depending on the values of parameters  $A$  and  $B$ , the solution of this equation describes both stable and unstable modes of the particle motion in the EDS volume. In the plane of the parameters ( $A, B$ ), there is a curve called the stability boundary separating the above regions. It is a major characteristic of the EDS; its approximate equation for the given configuration of the electrodes was first obtained in [7]:

$$B^2 = \frac{1}{8} (99 + 12A^2) - \frac{1}{4} \left[ \frac{1}{4} (99 + 12A^2)^2 - (1 + 4A^2) (81 + 36A^2) \right]^{1/2}. \quad (5)$$

At a fixed frequency of a.c. voltage  $f$  with increasing value of  $V_{a.c}$  the instability state is attained and the oscillation amplitude of the particle sharply increases. The value of this critical voltage can be measured with a high accuracy, which permits using Eq. (5) to determine the EDS characteristics by experiment as well as the sizes and other properties of the particles being investigated (the so-called "jumping-point method" [5]). The sizes of the particles used, determined from the investigation of the stability boundary of their motion in the EDS volume, are given in Table 1.

If a particle is disturbed from the equilibrium position at  $z = 0$  by changing the d.c. voltage  $V_{d.c}$ , it executes oscillations along the vertical axis of the suspension. In so doing, the oscillation amplitude, the displacement of the center of oscillations, and their phase give rich additional information about the physical characteristics of the microparticles (on the mass, density, charge, etc.) and the properties of the surrounding gas.

The nonlinear equation (3) was solved numerically by the finite-difference method. The authors also attempted to obtain its approximate analytical solution, using the Bubnov–Galerkin method of successive approximations. As the basis functions for the first approximation of the method, the functions  $\sin \tau$  and  $\cos \tau$  were chosen. Then the sought solution for  $z$  should be of the form

$$z = A_0 + a \sin \tau + b \cos \tau, \quad (6)$$

where  $A_0$ ,  $a$ , and  $b$  are the unknown coefficients to be determined. Substituting expression (6) into (3), we have

$$-a \sin \tau - b \cos \tau + aA \cos \tau - Ab \sin \tau - A_0B \cos \tau + ab \sin \tau \cos \tau + bB \cos^2 \tau - D = 0. \quad (7)$$

Multiplying (7) by the basis functions and integrating with respect to the whole period of oscillations, we obtain equations for determining the unknown coefficients  $a$  and  $b$ :

$$-a - Ab = 0, \quad -b - aA - A_0B = 0, \quad (8)$$

whence

$$a = \frac{A_0AB}{1 + A^2}, \quad b = -\frac{A_0B}{1 + A^2}. \quad (9)$$

From (9) it follows that the oscillation amplitude  $A_1$  and the oscillation phase  $\Theta$  are equal to

$$A_1 = (a^2 + b^2)^{1/2} = \frac{A_0B}{(1 + A^2)^{1/2}}, \quad \Theta = \arctan \frac{a}{b} = \arctan (-A). \quad (10)$$

The displacement of the oscillation center of the particle (center shift)  $A_0$  can be found from the following reasoning. We write expression (6) in the form

$$z = A_0 + A_1 \cos (\tau - \theta), \quad \sin \theta = \frac{a}{A_0}, \quad \cos \theta = \frac{b}{A_0}. \quad (11)$$

Substituting (11) into (3) and using the familiar trigonometrical formulas, we obtain

$$A_0 = \frac{D}{B^2} (1 + A^2). \quad (12)$$

Formulas (10) and (11), in view of the notations of (4), describe in the first approximation the motion of a charged aerosol particle in an EDS of the given configuration and can be used to determine experimentally its characteristics from the observations of the features of oscillations.

**Experimental Results.** Changing the value and frequency of a.c. voltage and the value of d.c. voltage in the EDS, one can verify the adequacy of the above theory to the experiment. Below, the principal results of such a comparison are given. Figure 3 shows the theoretical curve of the stability boundary and its experimental values for parti-

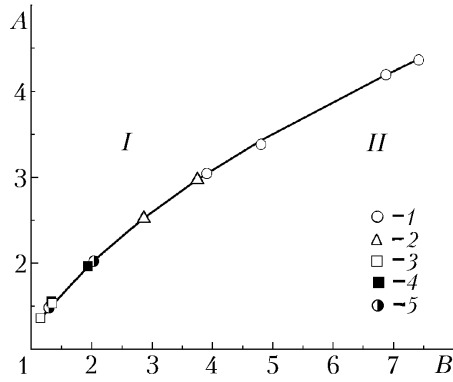


Fig. 3. Stability diagram of particle motion in the EDS (theory and experiment) (I and II, regions of stable and unstable motion): 1) lycopodium particles; 2) nickel; 3) iron; 4) titanium; 5) copper; curve, numerical solution of Eq. (3).

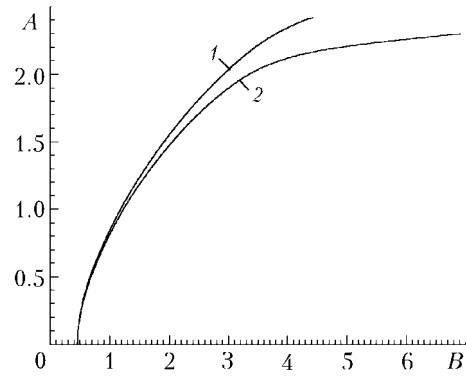


Fig. 4. Comparison of the stability boundary curves: 1) results of [7] (Eq. (5)); 2) solution of Eq. (3) by the numerical finite-difference method.

TABLE 2. Calculation of the Experimental Values of  $A_0$  and  $A_1$  with the Theoretical Calculation (3) by the Finite-Difference Method and the Theory by the Bubnov–Galerkin Method (10), (12) for the Lycopodium Particle with  $R_p = 13 \mu\text{m}$ ,  $V_{d.c}(0) = 25.0 \text{ V}$

$f$ , Hz	$V_{a.c.}$ , V	$V_{d.c.}$ , V	$A$	$B$	$\frac{A_{1num}}{A_{1exp}}$	$\frac{A_{1theor}}{A_{1exp}}$	$\frac{A_{0num}}{A_{0exp}}$	$\frac{A_{0theor}}{A_{0exp}}$
50	799	60.60	1.568	1.919	1.09	0.90	1.03	0.73
60	805	60.60	1.307	1.342	1.04	0.94	1.02	0.85
70	810	72.04	1.120	0.992	1.07	1.01	1.00	0.91
70	633	60.60	1.120	0.776	1.09	1.05	0.99	0.93
70	960	72.04	1.120	1.176	1.07	1.00	0.97	0.84
70	1080	48.96	1.120	1.323	1.02	0.97	1.00	0.82

cles of various substances and sizes. The lycopodium spores and the nickel particles obtained by the method of expressive dispersion of wires had a spherical shape, which permitted correct determination of their true radius. For other (nonspherical) particles, the effective aerodynamic radius has been determined. Note that there is a good agreement between the experimental data and the theoretical curve for particles of various substances and sizes.

Figure 4 gives a comparison of the results for the stability boundary curve obtained in [7] and in the numerical calculation of Eq. (3) by the finite-difference method. It is seen that the calculated curve coincides with the results of [7] when the parameter  $A$  is changed from 0 to 1. At  $A > 1$  discrepancies arise and they become significant at  $A \approx 2$ . Obviously, to analyze the experimental data at  $A > 2$ , it is expedient to use the results of the numerical calculation.

From relation (5) it follows that at  $A = 0$  the parameter  $B = 0.45416$  is a constant whose value can be used to determine experimentally the  $C_{a.c.}/C_0$  ratios from Eq. (4). Note that the value of  $A$  tends to zero either at a high frequency of the driving force or at very low gas pressures. For the EDS variant under investigation,  $C_{a.c.}/C_0 = (600 \pm 20) \text{ m}^{-1}$  has been obtained, which is in good agreement with the above estimates of this ratio for electrical parameters.

The oscillation amplitude and the oscillation center displacement have been measured for various values of the electric field parameters. Table 2 compares the experimental values for the amplitude  $A_1$  and displacement  $A_0$  with the values obtained by the numerical calculation by formulas (10) and (12). From Table 2 it is seen that the experimental values of  $A_0$  and  $A_1$  are in a better agreement with the numerical calculation than with the approximate theory, and an increase in the accuracy of numerical calculations thereby does not lead to an appreciable change in the values ob-

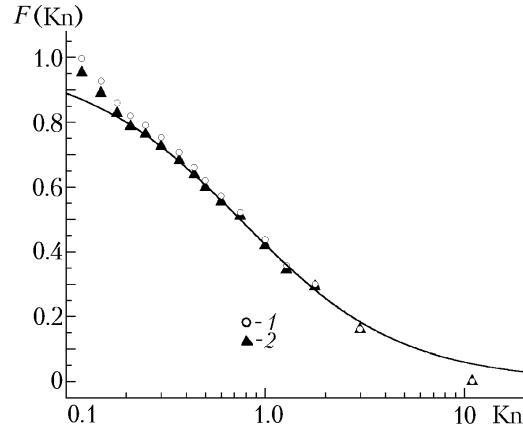


Fig. 5. Experimental determination of the  $F(Kn)$  correction for the drag force (Eq. (13)) from the investigation of the stability boundary for the lycopodium particle with  $R_p = 13.9 \mu\text{m}$  at  $f = 50 \text{ Hz}$ : 1) calculation with the use of (5) [7]; 2) calculation with the use of the numerical solution of (3) by the finite-difference method; curve, result of (14) [8].

tained. The disagreement with the theoretical values obtained by formulas (10) and (12) is likely to be due to the error of the first approximation of the Bubnov–Galerkin method.

For the first time, investigations of the particle-motion stability for various gas pressures in the EDS chamber have been carried out. It turns out that when the particle is moving at a constant frequency of the driving force, the parameter  $A$  depends on the gas pressure in the measuring chamber, and in so doing, it decreases with decreasing pressure. This fact can be explained correctly, taking into account the dependence of the drag force of a particle of invariable radius on the rarefied gas pressure. Indeed, the drag force of a particle of radius  $R_p$  can be given in the form [8]

$$F_d = 6\pi\eta R_p F(Kn) \frac{dz}{dt}, \quad (13)$$

where the dimensionless function  $F(Kn)$  takes into account the dependence of the drag force on the degree of rarity of the gas (Knudsen number). At a total accommodation of the energy and pulse of the gas molecules on the particle surface it is well approximated by the following familiar equation [8]:

$$F(Kn) = \frac{0.619}{Kn + 0.619} \left( 1 + \frac{0.310 Kn}{Kn^2 + 1.152 Kn + 0.785} \right). \quad (14)$$

Figure 5 gives a comparison between the theoretical results for  $F(Kn)$  obtained by formula (14) and the experimental data obtained from the investigation of the particle-motion stability at lower gas pressures. It is seen that there is good agreement between the theoretical and experimental results for small measurement errors. The deviations of the experimental data from theoretical predictions for small  $Kn$  are likely to be due to the inertial effects in the particle motion in this region (insufficiently small Reynolds numbers, which is meant in the theory of [8]) and at large  $Kn$  — to the necessity of taking into account in (14) the incomplete accommodation of the tangential pulse of the gas molecules under their interaction with the particle surface.

## CONCLUSIONS

In the present paper, the structure of the electrodynamic suspension with double plane-parallel electrodes is described. The proposed structure of the EDS has a number of advantages over suspensions of other types, including the one used by the author earlier [6]:

1) ease of preparation of electrodes (rings and disks) compared to electrodes of an intricate (e.g., hyperbolic) shape;

2) convenience of observing a particle and the possibility of realizing an external force action on it (electromagnetic radiation, temperature gradient, etc.);

3) optimum shape of electrodes for measuring vertical forces of various origin acting on the particle.

The developed theory of oscillatory particle motion in the EDS makes it possible to visualize the dependence of the results obtained on the factors acting on the particle. In one set of experiments with a concrete particle, a wide complex of its microphysical characteristics and properties of the surrounding gas can be determined simultaneously. We are planning to use this method in the future in investigating the phosphoretic and thermoconvective forces acting on aerosol particles.

This work was supported by the Russian Basic Research Foundation (grant No. 01-01-96451).

## NOTATION

$d$  and  $R_0$ , thickness and radius of electrodes-rings, m;  $D_0$ , diameter of electrodes-disks, m;  $h$  and  $H$ , distance between electrodes-rings and electrodes-disks, m;  $m$ , mass of the aerosol particle, kg;  $R_p$ , effective aerodynamic radius of the particle, m;  $q$ , particle charge, C;  $F_d$ , drag force of the particle, N;  $F(\text{Kn})$ , dimensionless function for the drag force;  $\text{Kn}$ , Knudsen number;  $z$ , axial component in the cylindrical system of coordinates, m;  $\eta$ , coefficient of dynamic viscosity of gas, Pa·sec;  $g$ , free-fall acceleration,  $\text{m/sec}^2$ ;  $\omega$ , circular frequency of the variable electric field, rad/sec;  $f$ , oscillation frequency of the variable electric field, Hz;  $t$ , time, sec;  $\tau$ , dimensional time constant in Eq. (6);  $E_{a.c}$  and  $E_{d.c}$ , variable and constant electric field strengths, V/m;  $E_{d.c}(0)$ , constant electric field strength at the EDS center, V/m;  $A$ ,  $B$ , and  $D$ , parameters of viscous drag, electric field, and external actions;  $C_{a.c}$  and  $C_0$ , geometric constants of the EDS;  $a$  and  $b$ , coefficients in Eq. (6);  $A_0$ , displacement of the oscillation center of the particle, m;  $A_1$ , particle oscillation amplitude, m;  $\Theta$ , phase of particle oscillations, rad;  $\theta$ , particle oscillation phase shift. Subscripts: p, particle; d, drag; a.c, alternating current; d.c, direct current; num, numerical; theor, theoretical; exp, experimental.

## REFERENCES

1. E. J. Davis, *Aerosol Sci. Technol.*, **26**, No. 3, 212–254 (1997).
2. R. F. Wuerker, H. Shelton, and R. V. Langmuir, *J. Appl. Phys.*, **30**, No. 3, 342–349 (1959).
3. J. Zhu, F. Zheng, M. L. Laucks, and E. J. Davis, *J. Colloid Interface Sci.*, **249**, No. 2, 351–358 (2002).
4. E. J. Davis, M. F. Buehler, and T. L. Ward, *Rev. Sci. Instrum.*, **61**, No. 4, 1281–1288 (1990).
5. F. Zheng, M. L. Laucks, and E. J. Davis, *J. Aerosol Sci.*, **31**, No. 10, 1173–1185 (2000).
6. V. A. Runkov, P. E. Suetin, and S. A. Beresnev, in: *Metastable States and Phase Transitions* [in Russian], Coll. Sci. Papers of the Institute of Thermophysics of the Ural Branch of the Russian Academy of Sciences, Ekaterinburg, Issue 4 (2000), pp. 102–113.
7. A. Muller, *Ann. Phys.*, **7**, No. 6, 206–220 (1960).
8. S. A. Beresnev, V. G. Chernyak, and G. A. Fomyagin, *J. Fluid Mech.*, **219**, 405–421 (1990).